A Node-Assigned PINN Model for Coupled Heat Transfer Calculations in a PWR Hot Channel

Fabiano Thulu and Zeyun Wu

Department of Mechanical and Nuclear Engineering, Virginia Commonwealth University, Richmond, VA 23284-3015 USA,
thulufg@vcu.edu, zwu@vcu.edu

https://doi.org/10.13182/(suffix to be created by ANS)

INTRODUCTION

The safety and reliability of Nuclear Power Plants (NPPs) rely heavily on thermal-hydraulic (T/H) system codes for accident analysis and regulatory compliance. Historically, T/H codes such as RELAP, MELCOR, and MAAP have been widely used in nuclear safety assessments. While these codes are highly robust, they depend on complex empirical correlations and a mix of implicit or explicit numerical formulations that may not always be fully consistent [1]. Such traditional methods often result in unidirectional coupling, in which multi-physics phenomena, such as the interaction between fuel rod heat conduction and coolant fluid dynamics, are solved sequentially rather than simultaneously. This treatment can introduce numerical diffusion and stability limitations, particularly during rapid evolving transients scenarios [2].

In recent years, physics-informed neural networks (PINNs) have emerged as a transformative approach for scientific computing [3]. By embedding governing partial differential equations (PDEs) directly into the loss function of deep learning models, PINNs can solve complex physical problems within a continuous differentiable framework [4]. However, the direct application of *vanilla* PINNs to full-scale reactor systems remains challenging due to strong spatial heterogeneity in the governing equations across different reactor components [5]. To address this limitation, the node-assigned physics-informed neural network (NA-PINN) approach assigns dedicated neural sub-networks to individual physical nodes such as volumes and junctions, thereby closely mirroring the nodalization strategy employed in traditional T/H codes [6]. In this work, we adopt and further develop the NA-PINN architecture, building upon the recently proposed framework in Ref. [7]. Specifically, we extended the NA-PINN methodology from its initial demonstration in MELCOR-based water tank models to aRELAP5-3D hot channel configuration with fully coupled fuel-cladding-coolant physics.

For the case study presented in this work, we focused on the T/H coupling in a pressurized water reactor (PWR) during cold-leg break transient. The analysis isolates the reactor hot channel and its associated fuel-rod heat structures. To integrate the heat structures , radial heat conduction equations for fuel pellets and cladding are embedded directly into the NA-PINN loss function. This integration addresses the thermal coupling gap identified in previous pilot studies [8]. To model single-phase flow conditions, the NA-PINN architecture is adapted to handle the steep pressure and temperature gradients characteristics of cold-leg break transients. To ensure strict enforcement of physical constraints, the shifting method is employed to impose initial plant conditions, guaranteeing that the neural-network solution is fully consistent with the PWR steady-state conditions at the onset of the break.

To the best of our knowledge, no prior study has applied an NA-PINN framework to coupled fuel-cladding-coolant modeling of PWR cold-leg break transients. By demonstrating that NA-PINNs can accurately reproduce the complex T/H transient behavior predicted by RELAP, this work lays the foundation of real-time, physics-based accident diagnostic tools and accelerated safety-margin assessment capabilities in nuclear energy systems.

METHODOLOGY

Node-Assigned PINN (NA-PINN) Architecture

In this work, the NA-PINN system is decomposed into localized sub-networks (volume and heat structure) as follows: The fluid volume networks were dedicated by six axial volumes of the core coolant channel. Each network takes time as input and predicts pressure and temperature. The flow junction network, representing the internal junctions of core coolant channel, predicting fluid velocity. Figure 1 illustrate the coolant channel nodalization for the NA-PINN framework, including a heat structure network (radial grid of networks) that represents the fuel pellet, gap and cladding layers. These networks predict the temperature distribution.

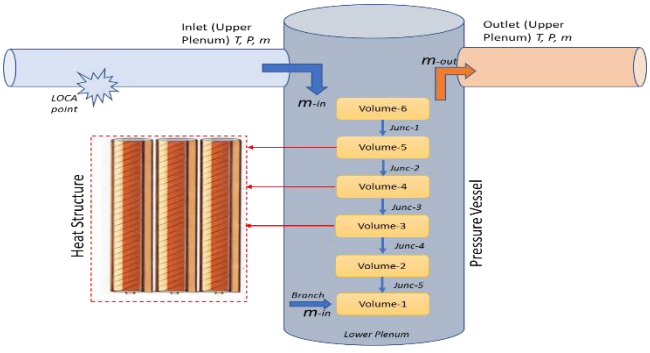

Fig. 1. Coolant Channel Nodalization for NA-PINN.

PINN Network Formulation

Governing Equations

For each axial volume in the reactor core, the T/H is governed by the conservation of energy. For the one phase flow during the initial stages of the cold-leg break transient, the rate of change of energy in the fluid volume is determined by the advection of enthalpy and the convective heat transfer from the cladding of the form

$$\rho_{f,i} V_i C_{p,f} \frac{dT_{f,i}}{dt} = \dot{m}_{in,i} C_{p,f} T_{f,i-1} - \dot{m}_{out,i} C_{p,f} T_{f,i} + h_i A_i \left(T_{s,i} - T_{f,i}\right) \quad (1)$$

The thermal behavior of the fuel rod cladding is governed by the balance between internal heat generation (fission and decay heat) and the heat removed by coolant in the form of

$$\rho_s V_{s,i} C_{p,s} \frac{dT_{s,i}}{dt} = Q_i - h_i A_i \left(T_{s,i} - T_{f,i}\right) \quad (2)$$

where Q_i is the volumetric heat source calculated from the reactor power distribution.

The Shifting Method for Hard Constraints

To ensure the simulation adheres to the initial steady state conditions defined in the PRW RELAP Input deck, we utilize the shift method. This method reformulates the neural network output $\mathcal{N}(t)$ into a physically constrained variable $\hat{u}(t)$ using the following additive equation:

$$\hat{u}(t) = \mathcal{N}(t) - \mathcal{N}(t_{start}) + u_{RELAP}(t_{start}) \quad (3)$$

The fluid temperature and mass flow rate boundary conditions (BCs) at volume 1 are constrained by the cold leg conditions. The heat flux at the cladding-coolant interface is enforced through the coupling term, which links the fluid and solid neural sub-networks in the form

$$q'' = h(T_s - T_f) \quad (4)$$

Physics-Informed Loss Formulation

For the NA-PINN network to capture transient behavior of the cold-leg break transient, a Mean Squared Error (MSE) loss is applied to the normalized temperature outputs for each node of the form

$$\mathcal{L}_{Data} = \frac{1}{N} \sum_{i=1}^{N} \left\| \hat{T}_i - T_{RELAP,i} \right\|^2 \quad (5)$$

where $\hat{T}_i$ is the predicted temperature for the volume i and $T_{RELAP,i}$ is the corresponding RELAP ground-truth.

We enforced the 1D conservation of energy equation. Since there is a single-phase liquid condition during the early blowdown, the residual is formulated in the form of

$$\mathcal{L}_{coolant} = \rho V C_P \frac{d\hat{T}}{dt} - \left[\sum \left(\dot{m} C_p T\right)_{in} - \sum \left(\dot{m} C_p T\right)_{out} + Q_{conv}\right] \quad (6)$$

The temporal derivative $\frac{d\hat{T}}{dt}$ is computed using automatic differentiation.

This heat structure module integrates the radial heat conduction and the loss function. The residual ensures that temperature change in cladding is balanced by the internal heat generation and heat flux of the fluid as

$$\mathcal{L}_{clad} = \rho_s V_s C_{P,s} \frac{d\hat{T}}{dt} - \left[Q - hA(\hat{T}_s - \hat{T}_f\right] \quad (7)$$

where Q represents the volumetric heat generation rate determined by the reactor power and decay heat curves.

The final composite loss function is weighted to balance data and physics terms in form as

$$\mathcal{L}_{Total} = \omega_D \mathcal{L}_{Data} + \omega_P (\mathcal{L}_{Coolant} + \mathcal{L}_{clad}) \quad (8)$$

Where ω_D is the data weight and $\omega_P$is the physics weight. The loss function was weighted using $\omega_D = 1.0$ and $\omega_P = 0.05$. This balance prevents the physics residuals (which involve high magnitude of power terms) from dominating the gradient descent.

We use the shifting method to ensure the model is starting from a calibrated steady-state, such that the predicted error is identically zero, regardless of the training state, by

$$\hat{T}(t) = NN(t) - NN(t_{100}) + T_{RELAP}(t_{100}) \quad (9)$$

Data Acquisition and Training Strategy

The baseline ground truth data is generated by running the RELAP5-3D for a generic PWR. The 12.85-inch cold leg break is considered for fast depressurization. Model building and training is performed with PyTorch using the Adam optimizer and an Exponential Linear Unit (ELU) activation function. This provides the necessary smoothness for calculating second-order derivatives in the heat conduction loss. Figure 2 illustrates the machine learning architecture employed in this work.

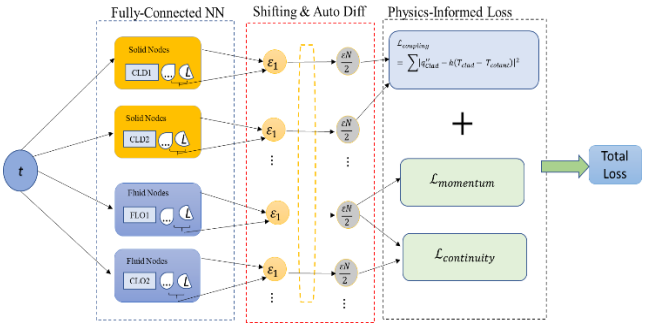

Fig. 2. the NA-PINN architecture

RESULTS AND DISCUSSION

At the starting stage (0 to 100 sec), all reactor parameters were relatively stable, indicating normal operation conditions. At the cold-leg break initiation (100 sec), all parameters begin to deviate significantly from their steady-state values. During the transient phase (100 – 850 sec) there is a rapid drop in pressure, followed by a stabilized at a much lower value. The coolant temperature initially drops due to rapid depressurization. It then exhibits fluctuations as the dominant heat transfer mechanisms change, with an overall trend towards lower temperature and a transition to a two-phase mixture. The mass flow rate significantly decreased, contributing a diminishing mass loss from the core. The fuel and clad temperature increase before eventually decreasing as decay heat reduces and emergency core cooling systems become effective.

The NA-PINN model predictions on the temperatures achieved a coefficient of determination of 0.9745 and 0.9859 and root mean squared error of 1.56 and 1.04 on the training and validation/test datasets, respectively. The observed behavior indicates that the vanilla NA-PINN model is capable of capturing the interactions and the underlining physics constraints in the model.

Figure 3 shows the training loss history. The training convergence was generally stable, with smooth decreasing and low total and physics losses. This result indicates a strong adherence to the governing physical laws. Minor oscillations in the data loss after 5000 epochs were attributed to optimizer transitions. This did not compromise overall model fidelity.

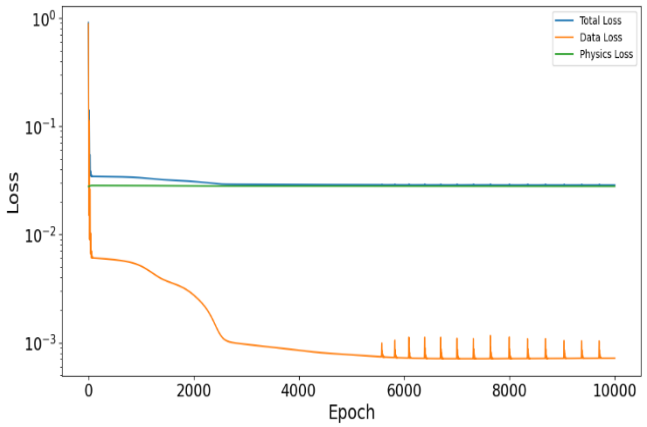

Fig. 3. NA-PINN training loss history.

Time series and spatial comparisons of ground true against model's predictions for void fraction, pressure, temperature and mass flowrate across transient phase and axial core volumes was performed. For example, Figure 4 and 5 show the predictions for different components by the NA-PINN model compared to the results directly obtained form RELAP5-3D simulations. The temperatures, pressure, void fraction and mass flow rates have shown an overall good agreement between the simulated and predicted values.

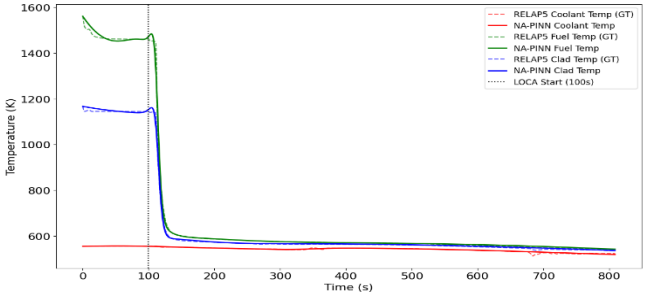

Fig. 4. Coolant, fuel and clad temperature transient.

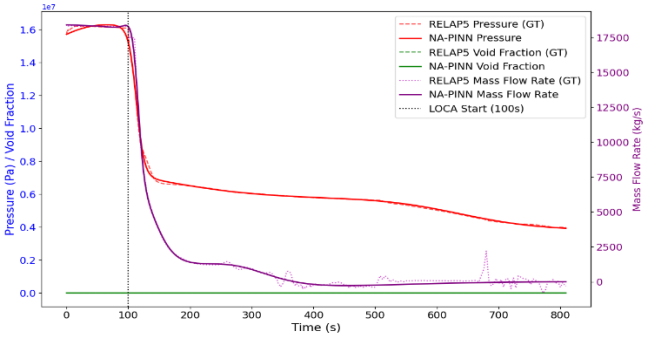

Fig. 5. Void fraction, pressure and mass flow rate transient.

Heatmap comparisons between ground truth and predictions also show a good spatial and temporal agreement across the core elevation and time domains. Figure 6 and 7 show the axial temperature distribution for cladding and coolant, respectively. As seen, the NA-PINN model captures the onset and propagation of the thermal gradients, following reactor state. It accurate reproduces the high-temperature zones and there downwards propagations for fuel clad temperature. Similarly, the cooling wave during the blowdown phase is visible, as the color shifts from red to blue across the axial core height. The NA-PINN model reproduces the spatial temperature distribution, including the hotter central volumes (node 3 and 4) that represent peak power regions in the hot channel.

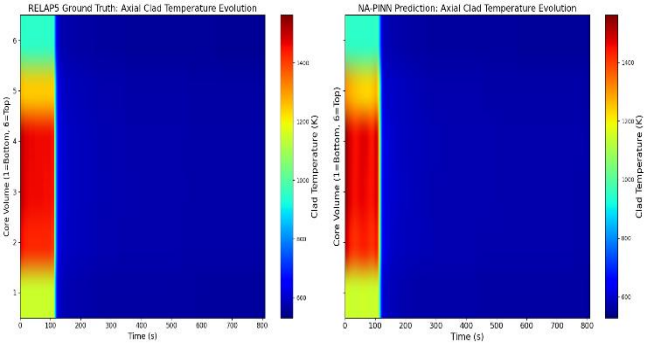

Fig. 6. Axial fuel clad temperature evolution.

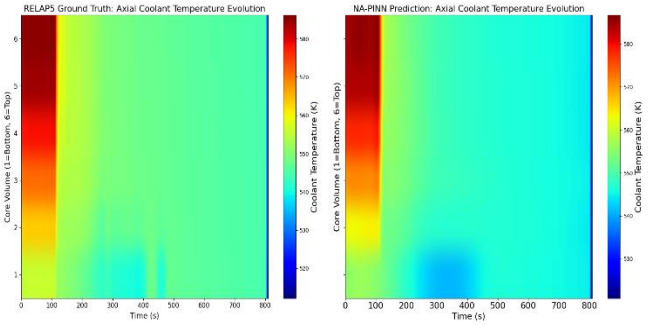

Fig. 7. Axial coolant temperature evolution.

Figure 8 and 9 show the fuel and cladding temparture profiles at some key stages in a comparaitve manner that in other figures. The comparative plots at t = 0 , 100 , 200 , 400 and 800 sec indicate that the NA-PINN model preserves a good thermal stratification and transient evolution predictions for fuel clad and coolant temperatures through the entire axial core volumes.

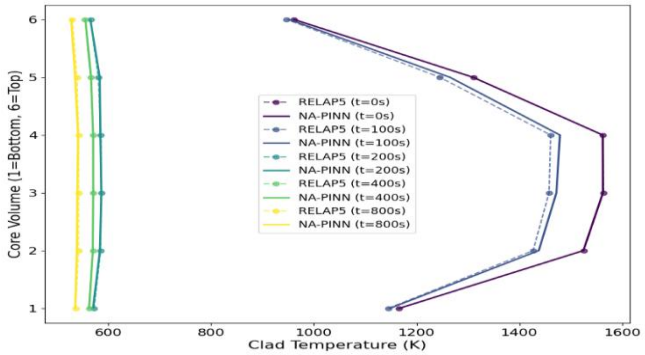

Fig. 8. Fuel clad temperature profiles at key stages.

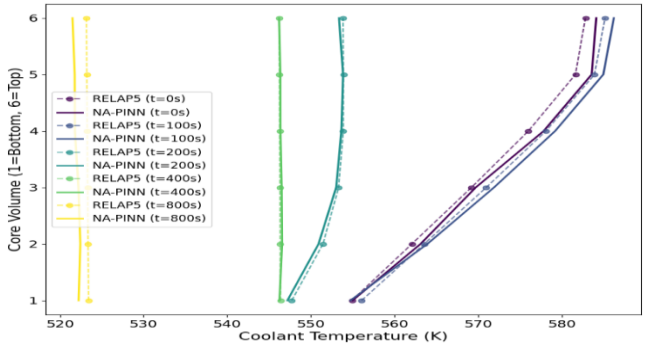

Fig. 9. Coolant temperature profiles at key stages.

CONCLUSIONS

In this work, we develop a node-adaptive physics-informed neural network (NA-PINN) for real-time simulation of cold-leg break transient. Independent neural networks are assigned to discrete axial control volume of the reactor core to circumvent the computational stiffness and convergence challenges commonly associated with central global networks in high-magnitude T/H systems. The proposed NA-PINN architecture demonstrates strong predictive performance for void fraction, temperature, pressure and mass flow rate for the cold-leg break transient.

The network successfully captures the global axial behavior of the reactor core, preserving physically consistent axial gradient. This preservation indicates the energy conservation residuals, expressed as $\dot{m}_{in}h_{in} - \dot{m}_{out}h_{in}$, are satisfied across volume boundaries. To extend this framework to a fully two-phase NA-PINN formulation, future work will incorporate mass quality and void fraction as output variables and modify the governing equations to explicitly account for steam-phase energy transport.

ACKNOWLEDGMENTS

This work was performed with the support of the U.S Department of Energy's Nuclear Energy University Program (NEUP) with the award No. DE-NE-0009505. This research has made use of the resources of the High-Performance Computing Center at Idaho National Laboratory, which is supported by the Office of the Nuclear Energy of the U.S Department of Energy and the National Science User Facilities under Contract No. DE-AC07-051D1517.

REFERENCES

1. F. G. D. THULU et al., "Safety Analysis in VVER-1000 Due to Large-Break Loss-of-Coolant Accident and Station Blackout Transient," *Nuclear Science and Engineering*, **196**, 568–583 (2021).
2. Q. LU et al., "Prediction method for thermal-hydraulic parameters of nuclear reactor system based on deep learning algorithm," *Applied Thermal Engineering*, **196**, 117272 (2021).
3. M. H. ELHAREEF and Z. WU, "Physics-Informed Neural Network Method and Application to Nuclear Reactor Calculations: A Pilot Study," *Nuclear Science and Engineering*, vol. **197**, 601–622 (2023)
4. Z. MAO et al., "Physics-informed neural networks for high-speed flows," *Computational Methods Applied Mechanical Engineering*, **360** (2020).
5. J. SHIN et al., "Node Assigned physics-informed neural networks for thermal-hydraulic system simulation: CVH/FL module," *Computer Science Language*, *Cornell University* (2025).
6. S. KHANAL et al., "Title: Comparison of CNN-based deep learning architectures for unsteady CFD acceleration on small datasets," *Computer Science*, *Cornell University* (2025).
7. R. SUN et al., "A physics-informed neural network framework for multi-physics coupling microfluidic problems," *Computational Fluids*, **284** (2024).
8. R. LAUBSCHER, "Simulation of multi-species flow and heat transfer using physics-informed neural networks, *Physics of Fluids*, **33** (2021).